Spin relaxation in ultracold spin-orbit coupled ⁴⁰K gas

T. Yu and M. W. Wu^*

Hefei National Laboratory for Physical Sciences at Microscale and Department of Physics, University of Science and Technology of China, Hefei, Anhui, 230026, China (Dated: October 31, 2018)

We report the anomalous D'yakonov-Perel' spin relaxation in ultracold spin-orbit coupled ⁴⁰K gas when the coupling between $|9/2, 9/2\rangle$ and $|9/2, 7/2\rangle$ states is much stronger than the spinorbit coupled field. Both the transverse and longitudinal spin relaxations are investigated with small and large spin polarizations. It is found that with small spin polarization, the transverse (longitudinal) spin relaxation is divided into four (two) regimes: the normal weak scattering regime, the anomalous D'yakonov-Perel'-like regime, the anomalous Elliott-Yafet-like regime and the normal strong scattering regime (the anomalous Elliott-Yafet-like regime and the normal strong scattering regime). With large spin polarization, we find that the Hartree-Fock self-energy, which acts as an effective magnetic field, can markedly suppress the transverse spin relaxation in both weak and strong scattering limits. Moreover, by noting that as both the momentum relaxation time and the Hartree-Fock effective magnetic field vary with the scattering length in cold atoms, the anomalous D'yakonov-Perel'-like regime is suppressed and the transverse spin relaxation is hence divided into three regimes in the scattering length dependence: the normal weak scattering regime, the anomalous Elliott-Yafet-like regime and the strong scattering regime. On the other hand, the longitudinal spin relaxation is again divided into the anomalous Elliott-Yafet-like and normal strong scattering regimes. Furthermore, it is found that the longitudinal spin relaxation can be either enhanced or suppressed by the Hartree-Fock effective magnetic field if the spin polarization is parallel or antiparallel to the effective Zeeman magnetic field.

PACS numbers: 03.75.Ss, 05.30.Fk, 67.85.-d

I. INTRODUCTION

Recently, the synthetic gauge fields in Bose and Fermi cold atom systems have been experimentally realized by laser control technique, which opens the door to study the spin-orbit coupling (SOC) and related phenomenon in these systems. 1-7 Much attention has been attractted to the spin-orbit coupled Bose-Einstein condensate⁵ and Fermi gas^{6,7} after the pioneering experimental works with precisely controlled SOC. In the spin-orbit coupled Bose-Einstein condensate, the SOC provides new possibilities to give rise to new quantum phases.^{8–16} In the ultracold Fermi gas system, the experimental realization of the spin-orbit coupled ⁴⁰K (Ref. 6) and ⁶Li (Ref. 7) systems provide a platform to simulate the spin dynamics in the solid state systems. Moreover, with tunable scattering strength between atoms by the Feshbach resonance, ¹⁷ the spin-orbit coupled ultracold Fermi gas can be used to study the influence of the interparticle interaction on the spin relaxation without being disturbed by disorders, inevitable in solid state systems. 18,19

The study of the spin-dynamics in the spin-orbit coupled Fermion gas has just started. Experimentally, in the $^{40}{\rm K}$ system, the lowest two magnetic sublevels $|9/2,9/2\rangle$ and $|9/2,7/2\rangle$, which are referred to as two spin-1/2 states, are coupled by a pair of Raman beams with the coupling strength $\Omega.^6$ In this system, the effective Hamiltonian including the SOC can be written as $(\hbar \equiv 1 \text{ throughout this paper})^{5-7,20}$

$$\hat{H}_0 = \varepsilon_{\mathbf{k}} + \mathbf{\Omega}(\mathbf{k}) \cdot \boldsymbol{\sigma}/2,\tag{1}$$

with the effective magnetic field

$$\mathbf{\Omega}(\mathbf{k}) = \left(\Omega, 0, -\delta - 2k_r k_x / m\right). \tag{2}$$

The first term $\varepsilon_{\mathbf{k}} = k^2/(2m)$ in Eq. (1) is the kinetic energy of atom with \mathbf{k} representing the center-of-mass momentum and m standing for the mass of the atom. $\Omega_z(\mathbf{k})$ in the second term is the effective magnetic field created by the Raman beams with k_r being the recoil momentum of the Raman beam and δ denoting the Raman detuning. σ is the vector composed of the Pauli matrices. It is noted that the coupling strength Ω acts as an effective Zeeman magnetic field along the $\hat{\mathbf{x}}$ -direction and the **k**-dependent effective magnetic field created by the Raman beams in Eq. (2) is perpendicular to the effective Zeeman magnetic field. Furthermore, δ can be set to be zero, which can be realized by tuning the Raman beams.⁵⁻⁷ It is interesting to see that the Hamiltonian Eq. (1) with $\delta = 0$ is similar to that of (110) semiconductor quantum wells with external magnetic field parallel to the \hat{x} -axis.²¹

Apart from the experimental investigations, the spin dynamics has been studied partly based on the effective Hamiltonian [Eq. (1)] theoretically. Tokatly and Sherman suggested that the polarized spin states are created by a weak effective Zeeman magnetic field, and the polarized spins relax to the equilibrium state due to the SOC and interatom collisions after swiching off the Zeeman magnetic field. ¹⁸ Natu and Das Sarma explored the spin dynamics of the two-dimensional, non-degenerate, harmonically trapped ultracold Fermi gas in the non-

interaction and diffusive limits, in the absence of the effective Zeeman magnetic field.¹⁹ They reported oscillations of the spin polarization in time domain and spin helix in space domain. So far, the spin dynamics with strong effective Zeeman magnetic field in the experimental feasibility has not been studied in the Fermi ultracold atom system.

The physics of the spin dynamics in the spin-orbit coupled 40 K gas in the presence of a strong effective Zeeman magnetic field can be very rich and intriguing. This can be conjectured from a very recent study by Zhou et al. on the spin dynamics in (110) quantum wells in the presence of a strong magnetic field **B** parallel to the \hat{x} -axis. There, due to the unique form of the effective magnetic field $\Omega(\mathbf{k})$, the spin relaxation may show anomalous scalings between the spin relaxation time (SRT) τ_s and momentum relaxation time τ_p^* for the transverse (longitudinal) spin relaxation with spins polarization perpendicular (parallel) to **B**, which is very different from the conventional situation with zero or small magnetic field.

In the conventional spin relaxation in n-type semi-conductors, the relevant spin relaxation mechanisms are the Elliott-Yafet (EY)^{22,23} and D'yakonov-Perel' (DP) mechanisms²⁴. In the EY mechanism, due to spin mixing, electron spins have a small chance to flip during each scattering, with the spin relaxation time (SRT) τ_s proportional to the momentum relaxation time τ_p^* . In the DP mechanism, the Dresselhaus²⁵ and/or Rashba²⁶ spin-orbit coupling (SOC) provide a **k**-dependent effective magnetic field $\Omega(\mathbf{k})$ and electron spins decay due to their precessions around this **k**-dependent effective magnetic field during the free flight between adjacent scattering events. Specifically, in the strong (weak) scattering limit when $\langle |\Omega(\mathbf{k})| \rangle \tau_p^* \ll 1$ ($\langle |\Omega(\mathbf{k})| \rangle \tau_p^* \gtrsim 1$), τ_s is inversely proportional (proportional) to τ_p^* .

Interestingly, in the work of Zhou et al., by varying the impurity density, the transverse (longitudinal) spin relaxation can be divided into four (two) regimes: the normal weak scattering regime ($\tau_{\rm s} \propto \tau_p^*$), the anomalous DP-like regime ($\tau_{\rm s}^{-1} \propto \tau_p^*$), the anomalous EY-like regime ($\tau_{\rm s} \propto \tau_p^*$) and the normal strong scattering regime ($\tau_{\rm s}^{-1} \propto \tau_p^*$) (the anomalous EY-like regime and the normal strong scattering regime).²¹ However, in the three-dimensional ultracold atom system, in spite of the similarity of the Hamiltonian, the interatom scattering, whose strength can also be tuned by the Feshbach resonance,¹⁷ is different from the impurity scattering. Whether the anomalous scalings in semiconductor systems are still valid is yet to be checked.

In the present work, with the interatom interaction explicitly included, we investigate the spin relaxation in the three-dimensional ultracold 40 K gas under the strong effective Zeeman magnetic field by the kinetic spin Bloch equation (KSBE) approach both analytically and numerically.²⁷ Interestingly, similar anomalous scalings between the SRT and momentum relaxation time are observed in the spin relaxation under strong effective Zeeman magnetic field satisfying $|\Omega| \gg \langle |\Omega_z(\mathbf{k})| \rangle$ when the

spin polarization is small by tuning the interatom scattering strength. $\langle ... \rangle$ here denotes the ensemble average. It is further revealed in this study that when the spin polarization is large, these anomalous relations are significantly influenced by the Hartree-Fock (HF) self-energy originating from the interatom interaction, acting as an effective magnetic field.^{27–31} It is shown that due to this HF effective magnetic field, the transverse spin relaxation can be suppressed. Consequently, in the scattering length dependence, by noting that both the momentum relaxation time and the HF effective magnetic field vary with the scattering length in cold atoms, the anomalous DP-like regime is suppressed and the transverse spin relaxation is hence divided into three instead of four regimes: the normal weak scattering regime, the anomalous EY-like regime and the strong scattering regime. On the other hand, the longitudinal spin relaxation can be either enhanced or suppressed by the HF effective magnetic field when the spin polarization is parallel or antiparallel to the effective Zeeman magnetic field and its scattering length dependence is again divided into the anomalous EY-like and normal strong scattering regimes. In addition, we find that the specific form of the effective magnetic field $\Omega(\mathbf{k})$ leads to a strong anisotropy between the transverse and longitudinal spin relaxations.

This paper is organized as follows. In Sec. II, we present the model and KSBEs. The main results are given in Sec. III. In Sec. III A, we solve the KSBEs analytically in a simplified model with the inelastic interatom scattering replaced by the elastic one and reveal the physics of the anomalous spin relaxation. In Sec. III B, with the inclusion of the interatom scattering, we numerically study the anomalous spin relaxation by varying the interatom scattering strength. The anisotropy of the transverse and longitudinal spin relaxations is also addressed in this part. We summarize in Sec. IV.

II. HAMILTONIAN AND KSBES

We start the investigation from the full Hamiltonian of the spin-orbit coupled ultracold atom systems, which is composed of the effective Hamiltonian \hat{H}_0 [Eq. (1)] and interaction interaction $\hat{H}_{\rm int}$, $^{19,32-35}$

$$\hat{H} = \hat{H}_0 + \hat{H}_{\text{int}}.\tag{3}$$

The interaction Hamiltonian \hat{H}_{int} can be written as $^{19,32-35}$

$$H_{\text{int}} = \frac{1}{2V} \sum_{\sigma=\uparrow,\downarrow} \sum_{\mathbf{k}_{1}+\mathbf{k}_{2}=\mathbf{k}_{3}+\mathbf{k}_{4}} g_{\sigma,\sigma} \Psi_{\mathbf{k}_{4},\sigma}^{\dagger} \Psi_{\mathbf{k}_{3},\sigma}^{\dagger} \Psi_{\mathbf{k}_{2},\sigma} \Psi_{\mathbf{k}_{1},\sigma}$$
$$+ \frac{g_{\uparrow,\downarrow}}{V} \sum_{\mathbf{k}_{1}+\mathbf{k}_{2}=\mathbf{k}_{3}+\mathbf{k}_{4}} \Psi_{\mathbf{k}_{4},\uparrow}^{\dagger} \Psi_{\mathbf{k}_{3},\downarrow}^{\dagger} \Psi_{\mathbf{k}_{2},\downarrow} \Psi_{\mathbf{k}_{1},\uparrow}. \quad (4)$$

Here $\Psi_{\mathbf{k},\sigma}$ is the annihilation operator of the atom with momentum \mathbf{k} in the spin- σ state with $\sigma \equiv \uparrow, \downarrow, V$ is the

volume of the system, and $g_{\uparrow,\downarrow} = 4\pi a/m$ is the scattering potential with a being the scattering length. The scattering potential $g_{\uparrow,\uparrow}$ and $g_{\downarrow,\downarrow}$ are set to be $g^{32,35}$

The KSBEs, derived via the nonequilibrium Green function method with the generalized Kadanoff-Baym Ansatz, ^{27,28,36–38} are utilized to study the spin relaxation in the ultracold Fermi gas:

$$\partial_t \rho_{\mathbf{k}}(t) = \partial_t \rho_{\mathbf{k}}(t)|_{\text{coh}} + \partial_t \rho_{\mathbf{k}}(t)|_{\text{scat}}.$$
 (5)

In these equations, $\rho_{\mathbf{k}}(t)$ represent the density matrices of atom with momentum \mathbf{k} at time t, in which the diagonal elements $\rho_{\mathbf{k},\sigma\sigma}$ describe the atom distribution functions and the off-diagonal elements $\rho_{\mathbf{k},\sigma-\sigma}$ represent the spin coherence for the inter spin-band correlation. In the collinear space, the coherent term is given by

$$\partial_t \rho_{\mathbf{k}}(t)|_{\text{coh}} = -i \left[\mathbf{\Omega}(\mathbf{k}) \cdot \boldsymbol{\sigma} / 2 + \Sigma_{\text{HF}}, \rho_{\mathbf{k}}(t) \right],$$
 (6)

where $\Sigma_{\mathrm{HF}} = -g \sum_{\mathbf{k}'} \rho_{\mathbf{k}'}$ is the HF self-energy and [,] denotes the commutator. The scattering terms $\partial_t \rho_{\mathbf{k}}(t)|_{\text{scat}}$ represent the interatom scattering. In our study, we focus on the situation that the effective Zeeman splitting energy and the SOC energy are much smaller than the Fermi energy and hence the scattering terms $read^{39}$

$$\begin{aligned} &\partial_{t}\rho_{\mathbf{k}}(t)|_{\text{scat}} \\ &= -\pi g^{2} \sum_{\mathbf{k'},\mathbf{k''}} \delta(\varepsilon_{\mathbf{k'}} - \varepsilon_{\mathbf{k}} + \varepsilon_{\mathbf{k''}} - \varepsilon_{\mathbf{k''}-\mathbf{k}+\mathbf{k'}}) \\ &\times \left[\rho_{\mathbf{k'}}^{>} \rho_{\mathbf{k}}^{<} \text{Tr}(\rho_{\mathbf{k''}-\mathbf{k}+\mathbf{k'}}^{<} \rho_{\mathbf{k''}}^{>}) - \rho_{\mathbf{k'}}^{<} \rho_{\mathbf{k}}^{>} \text{Tr}(\rho_{\mathbf{k''}-\mathbf{k}+\mathbf{k'}}^{>} \rho_{\mathbf{k''}}^{<}) \right] \\ &+ \text{H.c..} \end{aligned}$$

with $\rho_{\mathbf{k}}^{\leq} = \rho_{\mathbf{k}}$ and $\rho_{\mathbf{k}}^{\geq} = 1 - \rho_{\mathbf{k}}$. By solving the KSBEs, one obtains the SRT from the time evolution of the spin polarization P(t) = $\sum_{\mathbf{k}} \text{Tr}[\rho_{\mathbf{k}}(t)\boldsymbol{\sigma} \cdot \hat{\mathbf{n}}]/n_a$ with $\hat{\mathbf{n}}$ standing for the spin polarization direction and n_a being the density of the ultracold atom. The initial condition is set to be

$$\rho_{\mathbf{k}}(0) = \frac{F_{\mathbf{k}\uparrow} + F_{\mathbf{k}\downarrow}}{2} + \frac{F_{\mathbf{k}\uparrow} - F_{\mathbf{k}\downarrow}}{2} \boldsymbol{\sigma} \cdot \hat{\mathbf{n}}, \tag{8}$$

where $F_{\mathbf{k}\sigma} = \{\exp[(\varepsilon_{\mathbf{k}} - \mu_{\sigma})/(k_B T)] + 1\}^{-1}$ is the Fermi distribution function at temperature T, with $\mu_{\uparrow,\downarrow}$ standing for the chemical potentials determined by the atom density $n_a = \sum_{\mathbf{k}} \text{Tr}[\rho_{\mathbf{k}}]$ and the initial spin polarization P(0).

III. RESULTS

In this section, we solve the KSBEs first analytically and then fully numerically. In order to reveal the physics of the anomalous spin relaxation under strong effective Zeeman magnetic field, we first investigate the spin relaxation in a simplified model analytically, with the inelastic interatom scattering replaced by the elastic one. The situations with both small and large spin polarizations are considered. Specifically, the effects of the HF effective magnetic field on the transverse and longitudinal spin relaxations are shown explicitly. Then we numerically study the anomalous spin relaxation with the genuine interatom scattering. The scattering strength dependence of the spin relaxation is discussed facilitated with a full understanding of the SRTs from the analytical model.

Analytical results

Before performing the numerical study by solving the KSBEs, we first investigate the spin relaxation in a simplified model by replacing the inelastic interatom scattering by the elastic one. The conventional spin relaxation determined by the DP mechanism under the weak effective Zeeman magnetic field with $|\Omega| \ll \langle |\Omega_z(\mathbf{k})| \rangle$ has been studied in semiconductors in the strong and weak scattering limits $\langle |\Omega_z(\mathbf{k})| \rangle \tau_p^* \ll 1$ and $\langle |\Omega_z(\mathbf{k})| \rangle \tau_p^* \gg 1$, respectively, ^{24,27,40–44} [this situation is schematically shown in Fig. 1(a)]. Accordingly, in the strong (weak) scattering limit, the SRT is inversely proportional (proportional) to the momentum relaxation time. Moreover, the influence of the HF effective magnetic field to the spin relaxation has been fully investigated.^{27–30,39} Specifically, the SRT can be effectively enhanced due to the suppression of the inhomogeneous broadening³⁶ [i.e., the **k**-dependent effective magnetic field $\Omega_z(\mathbf{k})$ by the HF effective magnetic field.^{28–30} Here, we focus on the spin relaxation under the strong effective Zeeman magnetic field satisfying $|\Omega| \gg \langle |\Omega_z(\mathbf{k})| \rangle$ [illustrated in Fig. 1(b)].

The KSBEs including the HF effective magnetic field can be written as 45

$$\partial_{t}\rho_{\mathbf{k}} + i\left[\frac{\Omega_{z}(\mathbf{k})}{2}\sigma_{z}, \rho_{\mathbf{k}}\right] + i\left[\frac{\Omega}{2}\sigma_{x}, \rho_{\mathbf{k}}\right] + i\left[\frac{\Omega_{HF}}{2} \cdot \boldsymbol{\sigma}, \rho_{\mathbf{k}}\right] + \sum_{\mathbf{k}'} W_{\mathbf{k}\mathbf{k}'}(\rho_{\mathbf{k}} - \rho_{\mathbf{k}'}) = 0, \tag{9}$$

in which $W_{\mathbf{k}\mathbf{k}'} = 2\pi |U_{\mathbf{k}-\mathbf{k}'}|^2 \delta(\varepsilon_{\mathbf{k}} - \varepsilon_{\mathbf{k}'})$ describes the elastic scattering with $|U_{\mathbf{k}-\mathbf{k}'}|$ being the scattering matrix element. In our study, by considering the property of the interatom scattering potential [Eq. (4)], $|U_{\mathbf{k}-\mathbf{k}'}|$ is set to be constant g and hence $W_{\mathbf{k}\mathbf{k}'}$ is proportional to g^2 . $\Omega_z(\mathbf{k}) = \alpha k_x$ with $\alpha \equiv -2k_r/m$ is the **k**-dependent magnetic field and

$$\Omega_{\rm HF} = -2g \sum_{\mathbf{k}} \frac{1}{2} \text{Tr} \left[\rho_{\mathbf{k}} \boldsymbol{\sigma} \right] \equiv -2g \sum_{\mathbf{k}} \mathbf{S}_{\mathbf{k}}$$
(10)

acts as the HF effective magnetic field. It is noted that unlike that in semiconductors, ^{27,28}the HF effective magnetic field here is always proportional to the total spin vector $\mathbf{S} = \sum_{\mathbf{k}} \mathbf{S}_{\mathbf{k}}$.

1. SRT in the absence of HF effective magnetic field

When the spin polarization is small, i.e., the HF effective magnetic field is negligible, the total spin vector for

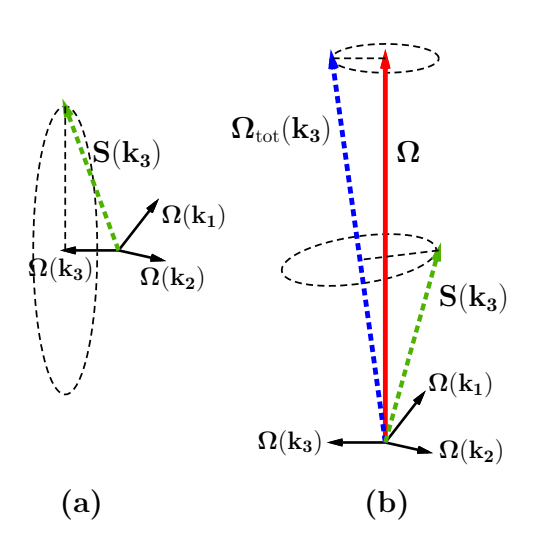


FIG. 1: (Color online) Schematic of the DP mechanism of the spin relaxation under the weak (a) and strong (b) effective Zeeman magnetic fields. Due to the random momentum scattering, the **k**-dependent magnetic field changes from $\Omega(\mathbf{k_1})$ to $\Omega(\mathbf{k_3})$ and the spin vector $\mathbf{S}(\mathbf{k})$ precesses around the **k**-dependent magnetic field during the free flight between adjacent scattering events. With the weak effective Zeeman magnetic field, this causes the conventional DP spin relaxation. With the strong effective Zeeman magnetic field satisfying $\Omega \gg \langle |\Omega(\mathbf{k})| \rangle$, $\Omega_{\rm tot}(\mathbf{k})$ is nearly parallel to the effective Zeeman magnetic field $\Omega = \Omega \hat{\mathbf{z}}$ and the DP spin relaxation shows anomalous behaviors.

the transverse and longitudinal spin relaxations can be obtained by solving the KSBEs [Eq. (9)] with large effective Zeeman magnetic field $|\Omega| \gg \langle |\Omega_z(\mathbf{k})| \rangle$ in the strong scattering limt $\langle |\overline{\Omega_z^2(\mathbf{k})}|/(2\Omega) \rangle \tau_{k,2} \ll 1$ (Ref. 21):⁴⁶

$$\mathbf{S}^{T}(t) \approx |\mathbf{S}^{T}(0)|e^{-t/\tau_{sz}} \left[\cos(\Omega t)\hat{\mathbf{z}} - \sin(\Omega t)\hat{\mathbf{y}}\right], \quad (11)$$

and

$$\mathbf{S}^{L}(t) \approx |\mathbf{S}^{L}(0)|\hat{\mathbf{x}}e^{-t/\tau_{sx}}.$$
 (12)

The corresponding transverse and longitudinal SRTs are

$$\tau_{\mathrm{s}z}^{-1} = \tau_{\mathrm{s}y}^{-1} = \left\langle \frac{\overline{\Omega_z^2(\mathbf{k})}^2 \tau_{k,2}}{4\Omega^2} + \frac{\overline{\Omega_z(\mathbf{k})}^2 \tau_{k,1}}{2(1 + \Omega^2 \tau_{k,1}^2)} \right\rangle, (13)$$

$$\tau_{sx}^{-1} = \left\langle \frac{\overline{\Omega_z(\mathbf{k})}^2 \tau_{k,1}}{1 + \Omega^2 \tau_{k,1}^2} \right\rangle, \tag{14}$$

in which $\overline{A_{\mathbf{k}}} = A_{\mathbf{k}} - \frac{1}{4\pi} \int d\omega_{\mathbf{k}} A_{\mathbf{k}}$ with $\omega_{\mathbf{k}}$ being the solid angle for momentum \mathbf{k} and the momentum relaxation time.

$$\tau_{k,l}^{-1} = \frac{m\sqrt{k}g^2}{2\pi} \int_0^{\pi} \sin\theta d\theta \left[1 - P_l(\cos\theta)\right],\tag{15}$$

with $P_l(\cos \theta)$ being the Legendre function. Obviously, the momentum relaxation time is inversely proportional to g^2 and hence a^2 , which can be tuned by the Feshbach resonance.¹⁷ Accordingly, the anomalous behavior of the transverse and longitudinal spin relaxations can be revealed.²¹

For the transverse spin relaxation, in the strong scattering limit, the SRT is limited by the competition of the two terms $\langle \overline{\Omega_z^2(\mathbf{k})}^2 \tau_{k,2}/(4\Omega^2) \rangle$ and $\langle \overline{\Omega_z(\mathbf{k})}^2 \tau_{k,1}/\left[2(1+\Omega^2\tau_{k,1}^2)\right] \rangle$ in Eq. (13). Specifically, when

$$\langle \overline{\Omega_z^2(\mathbf{k})}^2 \rangle \tau_{k,1} \tau_{k,2} / \langle 2 \overline{\Omega_z(\mathbf{k})}^2 \rangle \gg 1,$$
 (16)

the first term is dominant and the SRT $\tau_{sz} \approx \langle \overline{\Omega_z^2(\mathbf{k})}^2 \tau_{k,2}/(4\Omega^2) \rangle^{-1}$ is inversely proportional to the momentum relaxation time. It is further noted that when Eq. (16) is satisfied, for the situation under the weak effective Zeeman magnetic field, the system is in the weak scattering limit $[\langle |\Omega_z(\mathbf{k})| \rangle \tau_{k,1} \gg 1]$ with the SRT proportional to the momentum relaxation time. It is on this sense, this behavior under the strong effective Zeeman magnetic field is anomalous and this regime is referred to as the anomalous DP-like regime.²¹ When

$$\langle \overline{\Omega_z^2(\mathbf{k})}^2 \rangle \tau_{k,1} \tau_{k,2} / \langle 2 \overline{\Omega_z(\mathbf{k})}^2 \rangle \ll 1,$$
 (17)

the second term is dominant. If $\Omega \tau_{k,1}$ appearing in the denominator in the second term is much larger (smaller) than 1, the SRT $\tau_{sz} \approx \langle \overline{\Omega_z(\mathbf{k})}^2/(2\Omega^2\tau_{k,1})\rangle^{-1}$ ($\tau_{sz} \approx \langle \overline{\Omega_z(\mathbf{k})}^2\tau_{k,1}/2\rangle^{-1}$) is proportional (inversely proportional) to the momentum relaxation time. By noticing that the regime where Eq. (17) is satisfied is also in the strong scattering limit for the case of the weak effective Zeeman magnetic field ($\langle |\Omega_z(\mathbf{k})| \rangle \tau_{k,1} \lesssim 1$), where the SRT is inversely proportional to the momentum relaxation time, therefore, the behavior under the strong effective Zeeman magnetic field is anomalous (normal) when $\Omega \tau_{k,1} \gg 1$ ($\Omega \tau_{k,1} \ll 1$) and the system is in the anomalous EY-like (normal strong scattering) regime.²¹

For the transverse spin relaxation in the weak scattering limit, i.e., $\langle |\Omega_z^2(\mathbf{k})|/(2\Omega)\rangle \tau_{k,2} \gg 1$, the momentum scattering provides a spin relaxation channel and the SRT is positively proportional to the momentum relaxation time. The system is hence in the normal weak scattering regime.²¹

Therefore, with the decrease of the momentum relaxation time, the system experiences the normal weak scattering regime ($\tau_{sz} \propto \tau_{k,1}$), the anomalous DP-like regime ($\tau_{sz}^{-1} \propto \tau_{k,2}$), the anomalous EY-like regime ($\tau_{sz} \propto \tau_{k,1}$) and the normal strong scattering regime ($\tau_{sz}^{-1} \propto \tau_{k,1}$), successively [refer to Fig. 3(a)], with only the weak scattering regime being in the weak scattering limit. Accordingly, at the crossover between the normal weak scattering and anomalous DP-like regimes, a basin may appear with the position determined by

$$\langle |\overline{\Omega_z^2(\mathbf{k})}/(2\Omega)| \rangle \tau_{k,2} \approx 1;$$
 (18)

at the crossover between the anomalous DP- and anomalous EY-like regimes, a peak may arise with the position determined by

$$\tau_{k,1}\tau_{k,2} = \langle 2\overline{\Omega_z(\mathbf{k})}^2 \rangle / \langle \overline{\Omega_z^2(\mathbf{k})}^2 \rangle;$$
(19)

and at the crossover between the anomalous EY-like and normal strong scattering regimes, a basin may arise with the position determined by

$$\tau_{k,1} = \Omega^{-1}.\tag{20}$$

The analytical results for the tansverse spin relaxation rates $(1/\tau_s)$ with the effective Zeeman magnetic field and the momentum relaxation time in different regimes are summarized in the schematic diagram [Fig. 2 (a)].

For the longitudinal spin relaxation, from Eq. (14), when $\Omega\tau_{k,1} \gg 1$ ($\Omega\tau_{k,1} \ll 1$), the SRT $\tau_{sx} \approx \langle \overline{\Omega_z(\mathbf{k})}^2/(\Omega^2\tau_{k,1})\rangle^{-1}$ [$\tau_{sx} \approx \langle \overline{\Omega_z(\mathbf{k})}^2\tau_{k,1}\rangle^{-1}$] is proportional (inversely proportional) to the momentum relaxation time and the system is in the anomalous EY-like (normal strong scattering) regime [refer to Fig. 3(b)]. Moreover, there is no normal weak scattering regime due to the efficient suppression of the strong effective Zeeman magnetic field to the spin relaxation.²¹ Therefore, with the decrease of the momentum relaxation time, a basin may appear at the crossover between the anomalous EY-like and normal strong scattering regimes with the position determined by Eq. (20). The analytical results for the longitudinal spin relaxation rates with the effective Zeeman magnetic field and the momentum relaxation time in different regimes are summarized in the schematic diagram [Fig. 2 (b)].

2. SRT in the presence of HF effective magnetic field

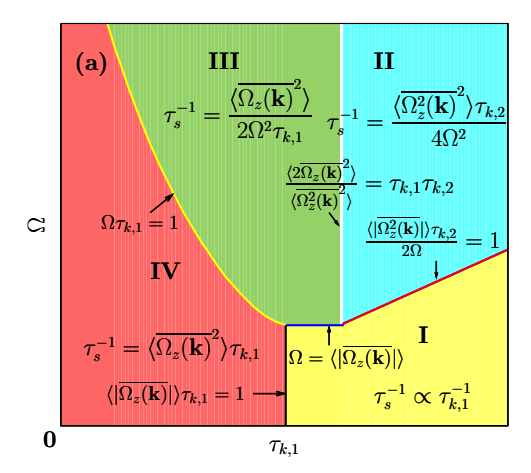
When the spin polarization is large, the HF effective magnetic field may influence the spin relaxation, as reported in semiconductors with weak Zeeman magnetic field. ^{28–31} To analytically reveal the effect of the HF effective magnetic field on the spin relaxation with strong Zeeman magnetic field in cold atoms, we discuss the situation with $|\Omega_{\rm HF}| \ll |\Omega|$, in which the total spin vector in Eq. (10) can be substituted by ${\bf S}^{\rm T}(t)$ [S^L(t)] [Eqs. (11) and (12)] for the transverse (longitudinal) spin relaxation. Accordingly, the HF effective magnetic field becomes a rotating magnetic field

$$\mathbf{\Omega}_{\mathrm{HF}}^{\mathrm{T}} = \Omega_{\mathrm{HF}}^{\mathrm{T}} \cos(\Omega t) \hat{\mathbf{z}} - \Omega_{\mathrm{HF}}^{\mathrm{T}} \sin(\Omega t) \hat{\mathbf{y}}, \qquad (21)$$

around the effective Zeeman magnetic field when the initial spin polarization is along the \hat{z} -axis and a static magnetic field

$$\mathbf{\Omega}_{\mathrm{HF}}^{\mathrm{L}} = \Omega_{\mathrm{HF}}^{\mathrm{L}} \hat{\mathbf{x}} \tag{22}$$

along the effective Zeeman magnetic field when the initial spin polarization is along the \hat{x} -axis, respectively. Here, $|\Omega_{\rm HF}|$ is the magnitude of the HF effective magnetic field.



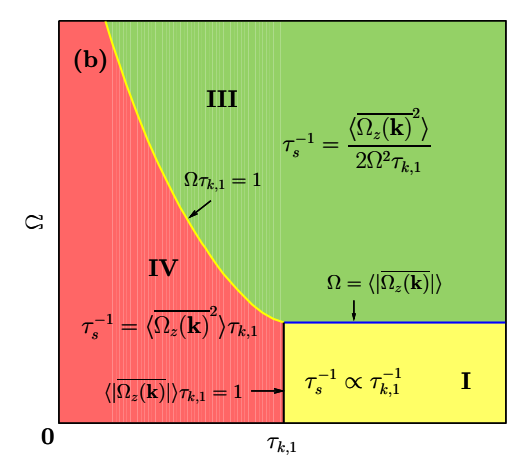


FIG. 2: (Color online) Schematic diagrams for the transverse (a) and longitudinal (b) spin relaxation rates with the effective Zeeman magnetic field and the momentum relaxation time. The Roman numbers represent different regimes of the spin relaxation: I, the normal weak scattering regime; II, the anomalous DP-like regime; III, the anomalous EY-like regime; IV, the normal strong scattering regime. The boundaries between the regimes I/II, II/III and III/IV are determined by Eqs. (18), (19) and (20), respectively. The boundaries between the regimes I/II and III/IV are determined by $\Omega = \langle |\Omega_z(\mathbf{k})| \rangle \text{ and } \langle |\Omega_z(\mathbf{k})| \rangle \tau_{k,1} = 1, \text{ respectively}.$

By solving the KSBEs [Eq. (9)] with the HF effective magnetic field [Eqs. (21) and (22)] included, one obtains the transverse and longitudinal SRTs. For the transverse spin relaxation, in the strong scattering limit $\langle \Omega_{\rm eff}(\mathbf{k}) \rangle \tau_{k,2} \ll 1$ with the condition $|\Omega_{\rm HF}| \gg \langle |\overline{\Omega_z^2(\mathbf{k})}/(2\Omega)| \rangle$, the SRT reads (the details of the derivation can be found in Appendix A)

$$\tau_{\mathrm{s}z}^{-1} = \left\langle \Omega_{\mathrm{eff}}^2(\mathbf{k}) \tau_{k,2} + \frac{\overline{\Omega_z(\mathbf{k})}^2 \tau_{k,1}}{2(1 + \Omega^2 \tau_{k,1}^2)} \right\rangle$$
 (23)

with

$$\Omega_{\rm eff}(\mathbf{k}) \equiv |\overline{\Omega_z^2(\mathbf{k})}|/(2\Omega\sqrt{1+\Omega_{\rm HF}^2\tau_{k,2}^2}). \eqno(24)$$

For the longitudinal spin relaxation, the static magnetic field is added directly to the effective Zeeman magnetic field, and the longitudinal SRT becomes

$$\tau_{\rm sx}^{-1} = \left\langle \frac{\overline{\Omega_z(\mathbf{k})}^2 \tau_{k,1}}{1 + (\Omega + \Omega_{\rm HF})^2 \tau_{k,1}^2} \right\rangle. \tag{25}$$

It is obvious that the SRTs in Eqs. (23) and (25) can be reduced back to Eqs. (13) and (14) when the HF effective magnetic field $\Omega_{\rm HF}=0$. With the inclusion of the HF effective magnetic field, both the transverse and longitudinal spin relaxations can be influenced. For the transverse situation, the spin relaxation can be suppressed; for the longitudinal situation, the spin relaxation can be either enhanced or suppressed when the HF effective magnetic field is parallel or antiparallel to the effective Zeeman magnetic field. Therefore, when the spin polarization is large, the behavior of the spin relaxation needs to be reanalyzed.

For the transverse spin relaxation, the HF effective magnetic field in Eq. (23) has very different influence on the spin relaxation depending on whether $|\Omega_{\rm HF}| \tau_{k,2} \ll 1$ or $|\Omega_{\rm HF}|\tau_{k,2}\gg 1$. When $|\Omega_{\rm HF}|\tau_{k,2}\ll 1$, the spin relaxation can also be divided into similar four regimes in the absence of $|\Omega_{HF}|$, but with some features modified. Specifically, the position of the peak [Eq. (19)] at the crossover between the anomalous DP- and anomalous EY-like regimes is modified to be $\tau_{k,1}\tau_{k,2} = \langle 2\overline{\Omega_z(\mathbf{k})}^2(1+$ $\Omega_{\rm HF}^2 \tau_{k,2}^2 \rangle / \langle \overline{\Omega_z^2(\mathbf{k})}^2 \rangle$. Therefore, due to the suppression of the inhomogeneous broadening by the HF effective magnetic field, the position of the peak shows up at weaker scattering. It is also noted that, with the second term in Eq. (23) being unchanged by $|\Omega_{HF}|$, the position of the basin [Eq. (20)] at the crossover between the anomalous EY-like and normal strong scattering regimes is also unchanged. However, when $|\Omega_{\rm HF}| \tau_{k,2} \gg 1$, the HF effective magnetic field may have strong influence on the spin relaxation, with the normal weak scattering and anomalous DP-like regimes being suppressed. This is because, in this situation, as $\langle \Omega_{\rm eff}(\mathbf{k}) \rangle \tau_{k,2} \approx \langle |\overline{\Omega_z^2(\mathbf{k})}| \rangle / (2\Omega\Omega_{\rm HF})$ is always much smaller than 1 when $|\Omega_{\rm HF}| \gg \langle |\overline{\Omega_z^2(\mathbf{k})}| \rangle / (2\Omega)$, the normal weak scattering regime is unreachable. Moreover, if $\langle \overline{\Omega_z^2(\mathbf{k})}^2 \rangle \tau_{k,1} \tau_{k,2}^{-1} / \langle 2\overline{\Omega_z(\mathbf{k})}^2 \Omega_{\mathrm{HF}}^2 \rangle \gg 1$, the first term in Eq. (23) is dominant and the SRT $\tau_{\mathrm{s}z} \approx$ $\langle \overline{\Omega_z^2(\mathbf{k})}^2/(4\Omega^2\Omega_{\mathrm{HF}}^2\tau_{k,2})\rangle^{-1}$ is proportional to the momentum relaxation time, showing the EY-like behavior. Hence the corresponding anomalous DP-like regime in the absence of the HF effective magnetic field becomes the anomalous EY-like regime. Accordingly, with the original anomalous EY-like and normal strong scattering regimes being unchanged, the spin relaxation is divided into the anomalous EY-like and normal strong scattering regimes.

For the longitudinal spin relaxation, the position of the basin Eq. (20) at the crossover between the anomalous EY-like and normal strong scattering regimes is modified to be $\tau_{k,1} = |\Omega + \Omega_{\rm HF}|^{-1}$. Therefore, with the HF effective magnetic parallel (antiparallel) to the effective magnetic field, the basin shows up at stronger (weaker) scattering when $|\Omega_{\rm HF}| \ll |\Omega|$.

B. Numerical results

In the previous simplified model (with the elastic scattering approximation), we are able to calculate the spin relaxation analytically under the strong effective Zeeman magnetic field, with the inclusion of the weak HF effective magnetic field satisfying $|\Omega_{\rm HF}| \ll |\Omega|$. However, for genuine system, the scattering is the inelastic interatom scattering. Moreover, the HF effective magnetic field can be tuned to be very strong ($|\Omega_{\rm HF}| \gtrsim |\Omega|$). In this section, we study the SRT by solving the KSBEs numerically. We focus on the scattering length dependence of the spin relaxation, with the scattering length being tuned by the Feshbach resonance.¹⁷

In the numerical calculation, the parameters we choose are within the experimental feasibility by referring to the experimental work of Wang et al.:6 The lowest two magnetic sublevels $|9/2, 9/2\rangle$ and $|9/2, 7/2\rangle$ are coupled by a pair of Raman beams with wavelength $\lambda = 773$ nm and the frequency difference $\omega/(2\pi) = 10.27$ MHz; The recoil momentum and energy are set to be $k_r = k_0 \sin(\theta/2)$ and $E_r = k_r^2 / 2m = 2\pi \times 8.34 \sin^2(\theta/2) \text{ kHz, with } k_0 = 2\pi/\lambda$ and θ denoting the angle between the two Raman beams. In our study, we choose $\sin(\theta/2) = 0.125$. The Raman detuning $\delta = \omega_z - \omega$ is set to be zero by choosing the Zeeman shift $\omega_z/(2\pi) = 10.27$ MHz. It is noted that with these parameters, the condition that the SOC energy is much smaller than the kinetic energy is satisfied. The scattering length varies from $0.01a_0$ to $50a_0$. Here, $a_0 = 169a_B$, with a_B being the Bohr radius, is taken from the experimental value.⁶ The Fermi momentum and the temperature are set to be $k_{\rm F}=32k_r$ and $T=0.2T_{\rm F}$ $(T_{\rm F}$ is the corresponding Fermi temperature), according to Wang et al.. The strengths of the effective Zeeman magnetic field Ω are taken to be $400E_r$ and $40E_r$, corresponding to $\Omega > \langle |\Omega_z(\mathbf{k})| \rangle$ and $\Omega < \langle |\Omega_z(\mathbf{k})| \rangle$, respec-

In Figs. 3(a) and (b), the transverse and longitudinal SRTs are plotted against the scattering length under strong and weak effective Zeeman magnetic fields, respectively, with both small and large spin polarizations P=1% and 100%. Below we analyze the transverse and longitudinal spin relaxations, separately.

1. Transverse spin relaxation

For the transverse spin relaxation, when the spin polarization is small (P = 1%), it is shown in Fig. 3(a) that the

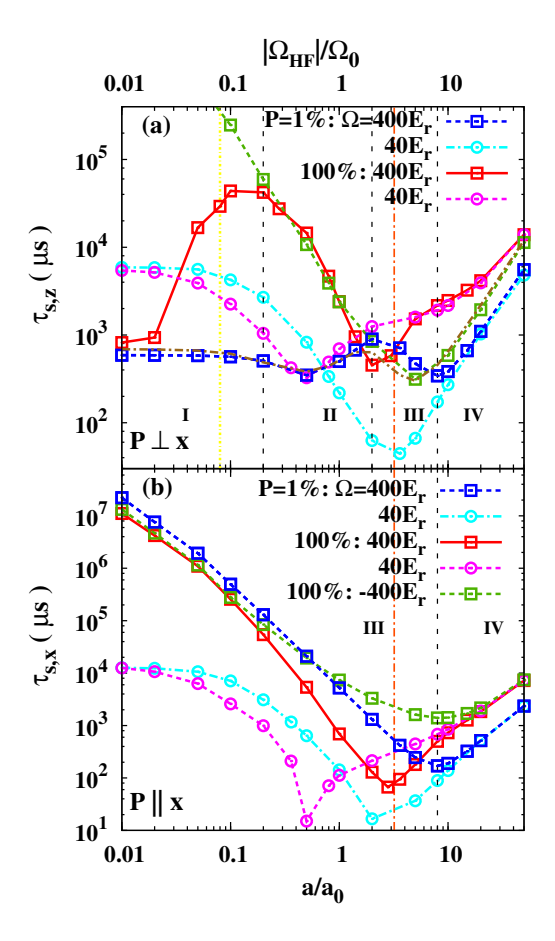


FIG. 3: (Color online) Transverse (a) and longitudinal (b) SRTs against the scattering length under both strong and weak effective Zeeman magnetic fields, with small and large spin polarizations P = 1% and 100%. The Roman numbers represent different regimes of the spin relaxation: I, the normal weak scattering regime; II, the anomalous DP-like regime; III, the anomalous EY-like regime; IV, the normal strong scattering regime. The vertical black dashed lines in (a) and (b) indicate the boundaries between different regimes for the transverse and longitudinal spin relaxations under the strong effective Zeeman magnetic field with P = 1%. The vertical orange (yellow) chain lines indicate the boundary between the weak and strong scattering regimes under the weak (strong) effective Zeeman magnetic field with P=1%(P = 100%). For the transverse situation (a), the green dashed curve with squares represents the SRT under the fixed HF field $|\Omega| = 75E_r$ and the gray chain curve shows the SRT in the absence of the HF field. For the longitudinal situation (b), $\Omega = 400E_r$ (-400 E_r) indicates the spin polarization is parallel (antiparallel) to the effective Zeeman magnetic field. We also plot the corresponding HF field $|\Omega_{\rm HF}|$ of the scattering length with P=100% (note the scale is on the top frame of the figure with $\Omega_0 = 240E_r$).

behavior of the spin relaxation under the strong effective Zeeman magnetic field is very different from the situation under the weak one. Under the strong effective Zeeman magnetic field, with the genuine interatom scattering, the anomalous behaviors of the transverse spin relaxation demonstrated in the simplified model are confirmed. Ac-

cordingly, the spin relaxation can be divided into four regimes: I, the normal weak scattering regime; II, the anomalous DP-like regime; III, the anomalous EY-like regime; and IV, the normal strong scattering regime.²¹ Moreover, the boundaries between the regimes I/II, II/III and III/IV can be determined by Eqs. (18), (19) and (20) (shown by the vertical black dashed lines), respectively. By noticing that $\tau_{k,1}$ and $\tau_{k,2}$ in these equations are in the same order, they can be replaced by τ_p^* limited by the interatom scattering approximately. Furthermore, by noting that the position of the basin between III and IV is at $a=8a_0$, where $\tau_p^*=\Omega^{-1}\propto a^{-2}$ is satisfied, we find $\tau_p^* = (8a_0/a)^2/\Omega$. Accordingly, from Eqs. (18) and (19), the boundaries between I/II and II/III are at $a \approx 0.2a_0$ and $a \approx 2a_0$, respectively, in good agreement with the numerical calculation in Fig. 3(a). For comparison, we also calculate the SRT under the weak effective Zeeman magnetic field. It can be seen from the figure that the spin relaxation can be divided into weak and strong scattering regimes (separated by the vertical orange chain line with $a \approx 3.2a_0$ by $\langle |\Omega_z(\mathbf{k})| \rangle \tau_p^* = 1$, which further confirms the investigation of the conventional spin relaxation in semiconductors under small magnetic field. $^{24,27,40-44}$

When the spin polarization is large (P = 100%) and hence with large HF effective magnetic field, it also can be seen from Fig. 3(a) that the behavior of the spin relaxation under the strong effective Zeeman magnetic field is very different from the situation under the weak one. In the presence of the strong effective magnetic field, the SRT shows a peak and a basin with the increase of the scattering length and can be divided into three regimes rather than four. Moreover, it seems that with large spin polarization, the normal weak scattering regime disappears and the peak (between II and III) and the basin (between III and IV) are shifted to the weaker scattering, with the SRT showing opposite trends in regimes I, II and III compared with the case of small spin polarization. However, if the HF effective magnetic field [Eq. (10)] is removed when P = 100% (the gray chain curve), the system also shows four regimes similar to the case of small spin polarization, with a small modification of the positions of the peak and the basin. This confirms that the anomalous behavior of the spin relaxation with large spin polarization is contributed by the HF effective magnetic field.

One notices that the numerical results at large spin polarization differs qualitatively from the analytical analysis in Sec. III A. In the analytical model, with the condition $|\Omega_{\rm HF}| \gg \langle |\overline{\Omega_z^2(\mathbf{k})}| \rangle/(2\Omega)$ satisfied, when $|\Omega_{\rm HF}|\tau_p^* \gg 1$ ($|\Omega_{\rm HF}|\tau_p^* \ll 1$), there are two (four) regimes for the spin relaxation. However, in the numerical study here, with $|\Omega_{\rm HF}|\tau_p^* \gg 1$ satisfied in regimes I-III (noting that with $a=0.1a_0$, $|\Omega_{\rm HF}|\tau_p^* \approx 400$ is much larger than 1), there are three instead of two regimes for the spin relaxation. This originates from the fact that in the analytical model, the HF effective magnetic field is fixed and much larger than $\langle |\overline{\Omega_z^2(\mathbf{k})}| \rangle/(2\Omega)$. However, here the HF effective magnetic field increases simultaneously with the

increase of the scattering length as $|\Omega_{\rm HF}| \propto a$ [Eq. (10)] and can be smaller or larger than $\langle |\Omega_z^2({\bf k})| \rangle/(2\Omega)$. For comparison, the case with a fixed HF effective magnetic field $|\Omega_{\rm HF}| = 75 E_r$ is plotted in the figure and one finds indeed two regimes appear. It is noted that with the varying HF effective magnetic field, the system can be divided into the weak and strong scattering regimes with the boundary determined by $\langle \Omega_{\rm eff}({\bf k}) \rangle \tau_p^* \simeq 1$ (shown by the vertical yellow chain line with $a \approx 0.08 a_0$). Below, we discuss the underlying physics in detail in the strong and weak scattering limits, respectively.

We first focus on the strong scattering limit. In this limit, as shown in Fig. 3(a), the SRT first decreases and then increases with the increase of the scattering length, showing the anomalous EY-like and normal strong scattering behaviors, respectively. These behaviors can be understood in the weak and strong HF effective magnetic field limits with $|\Omega_{\rm HF}| \ll |\Omega|$ and $|\Omega_{\rm HF}| \gg |\Omega|$, separately. In the weak HF effective magnetic field limit, corresponding to $a \ll 1.6a_0$ (noting that $|\Omega_{\rm HF}| \approx 400E_r$ when $a = 1.6a_0$, the behavior of the spin relaxation can be analyzed facilitated with the simplified model [Eq. (23)]. One notices that the first term in Eq. (23) is unchanged $(\Omega_{\rm HF}^2 \tau_p^* \propto a^0)$ and the second term decreases with increasing the scattering length. With $\langle \overline{\Omega_z^2(\mathbf{k})}^2 \rangle / \langle 2 \overline{\Omega_z(\mathbf{k})}^2 \rangle \lesssim \Omega_{\mathrm{HF}}^2$ in this regime satisfied, the second term in the SRT is dominant, giving the EY-like behavior in the scattering length dependence of the spin relaxation.⁴⁸ In the strong HF effective magnetic field limit $|\Omega_{\rm HF}| \gg |\Omega|$, corresponding to $a \gtrsim 10a_0$, with $|\Omega|\tau_p^* \ll 1$, the spin relaxation returns to the normal strong scattering regime $(\tau_s^{-1} \propto \tau_p^*)$, with the SRT increasing with the increase of the scattering length. Moreover, due to the strong HF effective magnetic field, the inhomogeneous broadening can be effectively suppressed in this normal strong scattering regime. ^{27–30,39} Therefore, the SRT in this regime is significantly enhanced compared to the situation with small spin polarization.

We then turn to the weak scattering limit. It is shown in Fig. 3(a) that with the increase of the scattering length, i.e., the HF effective magnetic field, the SRT is significantly enhanced. This is because in the presence of the strong effective Zeeman magnetic field, the inhomogeneous broadening is markedly suppressed by the HF effective magnetic field [Eq. (24)]. Consequently, a peak arises at the crossover of the weak and strong scattering limits.

For comparison, we also calculate the SRT with the weak effective Zeeman magnetic field. The spin relaxation can also be divided into conventional weak and strong scattering regimes, with the boundary shifted to the weaker scattering due to the suppression of the inhomogeneous broadening by the HF effective magnetic field. ^{27–30,39} In the strong scattering limit, the SRT is significantly enhanced by the HF effective magnetic field, which agrees with the results in semiconductors. ^{27–30,39} In the weak scattering limit, one observes that the SRT is suppressed compared to the situation with small spin

polarization. This is because with larger spin polarization, the population of the atoms in the **k**-space is broadened. Consequently, the inhomogeneous broadening for the spin relaxation is enhanced and the SRT is suppressed. 49

2. Longitudinal spin relaxation

For the longitudinal spin relaxation, when the spin polarization is small (P = 1%), it is shown in Fig. 3(b) that no matter the effective Zeeman magnetic field is strong ($|\Omega| = 400E_r$) or weak ($|\Omega| = 40E_r$), the SRTs always show a basin with the increase of the scattering length. 21,24,27,40-44 However, the underlying physics is very different. Under the strong effective Zeeman magnetic field, as revealed in the simplified model in Sec. III A, the spin relaxation can be divided into the anomalous EY-like and normal strong scattering regimes, with the boundary shown by the vertical black dashed line at $a = 8a_0$. However, under the weak effective magnetic field, the system is divided into conventional weak and strong scattering regimes (separated by the vertical purple chain line by $\langle |\Omega_z(\mathbf{k})| \rangle \tau_p^* = 1$, in agreement with the situation in semiconductors under the weak magnetic field. 21,24,27,40-44

When the spin polarization is large (P = 100%), the spin relaxations also present similar behaviors under the strong and weak effective Zeeman magnetic fields, showing a basin with the increase of the scattering length. In the presence of the strong effective Zeeman magnetic field, by noting that the HF effective magnetic field is antiparallel to the spin polarization [Eqs. (10)], when the spin polarization is parallel (antiparallel) to the effective Zeeman magnetic field, the total magnetic field $|\Omega + \Omega_{HF}|$ along the \hat{x} -axis is suppressed (enhanced) by the HF effective magnetic field. Accordingly, from Eq. (25), in which $|\Omega + \Omega_{\rm HF}|$ appears in the denominator, the SRT is suppressed (enhanced) when the spin polarization is parallel (antiparallel) to the effective Zeeman magnetic field, shown by the red solid (green dashed) curve with squares in the figure.

For comparison, we also calculate the SRT in the presence of weak effective Zeeman magnetic field. The spin relaxation can be divided into conventional weak and strong scattering regimes, with the position of the basin shifting to the weaker scattering due to the suppression of the inhomogeneous broadening by the HF effective magnetic field. In the strong scattering limit, the spin relaxation is suppressed due to the HF effective magnetic field. ^{27–30,39} In the weak scattering limit, similar to the transverse situation with weak effective Zeeman magnetic field, the SRT is suppressed due to the enhancement of the inhomogeneous broadening with large spin polarization.

3. Anisotropy of SRT

Finally, we analyze the anisotropy of the SRT under strong effective Zeeman magnetic field. By comparing the cases in the same conditions in Figs. 3(a) and (b), it is shown that the SRTs for the transverse and longitudinal spin relaxations are very different. When the spin polarization is small, there are four regimes for the transverse spin relaxation but only two regimes for the longitudinal situation. Specifically, at the normal strong scattering regime, the transverse SRT is two times as large as the longitudinal one. This anisotropy comes from the fact that under the unique effective magnetic field [Eq. (2)], the inhomogeneous broadening for the transverse and longitudinal spin relaxations are different, with the SRTs shown in Eqs. (13) and (14).²¹ When the spin polarization is large, there are three regimes for the transverse spin relaxation and again two regimes for the longitudinal one. In this situation, the HF effective magnetic field contributes to the anisotropy of the transverse and longitudinal spin relaxations.

IV. SUMMARY

In summary, we have investigated the spin relaxation in ultracold spin-orbit coupled ⁴⁰K gas under the strong effective Zeeman magnetic field $[|\Omega| \gg \langle |\Omega_z(\mathbf{k})| \rangle]$ both analytically and numerically. We find that when the spin polarization is small, the SRT shows anomalous scalings with the momentum relaxation time, with the transverse (longitudinal) spin relaxation divided into four (two) regimes in the scattering length dependence: the normal weak scattering regime $(\tau_s \propto \tau_p^*)$, the anomalous DP-like regime $(\tau_s^{-1} \propto \tau_p^*)$, the anomalous EY-like regime $(\tau_s \propto \tau_p^*)$ and the normal strong scattering regime $(\tau_s^{-1} \propto \tau_p^*)$ (the anomalous EY-like regime and the normal strong scattering regime). Specifically for the anomalous regime of the spin relaxation, in the transverse situation, there exists a regime, i.e., the anomalous DP-like (EY-like) regime in the conventional weak (strong) scattering limit showing anomalous spin relaxation behavior with the SRT inversely proportional (proportional) to the momentum relaxation time; in the longitudinal situation, the conventional weak scattering regime is suppressed by the strong effective Zeeman magnetic field and the system shows the EY-like behavior (i.e., the anomalous EY-like regime).

When the spin polarization is large, a large HF effective magnetic field shows up. We find that for the transverse spin relaxation, the HF effective magnetic field can efficiently enhance the SRT by suppressing the inhomogeneous broadening in both the weak and strong scattering limits. Moreover, it is noted that by varying the scattering length, both the momentum relaxation time and the HF effective magnetic field vary, but with $|\Omega_{\rm HF}|\tau_p^*$ fixed. Consequently, in the scattering length dependence of the spin relaxation, when $|\Omega_{\rm HF}|\tau_p^*\gg 1$, the anoma-

lous DP-like regime is suppressed and the transverse SRT is divided into three regimes: the normal weak scattering regime, the anomalous EY-like regime and the normal strong scattering regime. Specifically for the normal weak scattering regime, the SRT is inversely proportional to the momentum relaxation time due to the suppression of the inhomogeneous broadening by the HF effective magnetic field. On the other hand, for the longitudinal situation, with the inclusion of the HF effective magnetic field, the spin relaxation is again divided into two regimes: the anomalous EY-like regime and the normal strong scattering regime. Moreover, we find that the spin relaxation can be either enhanced or suppressed by the HF effective magnetic field if the spin polarization is parallel or antiparallel to the effective Zeeman magnetic field.

The physics of the anomalous DP spin relaxation under the strong effective Zeeman magnetic field revealed in this paper is rich and intriguing. Moreover, the conditions to observe these interesting phenomena are within the experimental feasibility in the ultracold spin-orbit coupled $^{40}{\rm K}$ gas. 6 Till now, what predicted in this investigation has not yet been experimentally reported and we expect that our work will cause more experimental investigations.

Acknowledgments

The authors would like to thank E. Ya. Sherman for bringing this problem into our attention. One of the authors (TY) would like to thank Y. Zhou for valuable discussions. This work was supported by the National Natural Science Foundation of China under Grant No. 11334014, the National Basic Research Program of China under Grant No. 2012CB922002 and the Strategic Priority Research Program of the Chinese Academy of Sciences under Grant No. XDB010000000.

Appendix A: Analytical analysis of the transverse SRT with the HF effective magnetic field

We analytically derive the transverse SRT based on the KSBEs [Eq. (9)] including the HF rotating magnetic field [Eq. (10)] under the elastic scattering approximation. When the strong effective Zeeman magnetic field satisfies $|\Omega| \gg \langle |\Omega_z(\mathbf{k})| \rangle$, it is convenient to solve the KSBEs in the helix space. In the helix space, we further transform the KSBEs into the interaction picture and use the rotation wave and Markovian approximations. ^{38,50}

In the collinear space, the density martix can be expanded by the spherical harmonics function $Y_l^m(\theta_{\mathbf{k}}, \phi_{\mathbf{k}})$

$$\rho_{\mathbf{k}} = \sum_{l,m} \rho_{k,l}^m Y_l^m(\theta_{\mathbf{k}}, \phi_{\mathbf{k}}), \tag{A1}$$

with $\theta_{\mathbf{k}}$ ($\phi_{\mathbf{k}}$) being the zenith (azimuth) angle between \mathbf{k} and \hat{x} -axis (\hat{y} -axis in the \hat{y} - \hat{z} plane). Furthermore,

by noting that the scattering term can be written as $\sum_{l,m} \rho_{k,l}^m Y_l^m(\theta_{\mathbf{k}}, \phi_{\mathbf{k}})/\tau_{k,l}$ [$\tau_{k,l}$ is defined in Eq. (15)] and the **k**-dependent magnetic field $\Omega_z(\mathbf{k})$ depends only on the zenith angle $\theta_{\mathbf{k}}$, the kinetics of the density martrix with m=0 in the KSBEs is independent on the ones with $m \neq 0$. Therefore, we can define the quantity

$$\rho_{\mathbf{k}}^* = \frac{1}{2\pi} \int_0^{2\pi} d\phi_{\mathbf{k}} \, \rho_{\mathbf{k}},\tag{A2}$$

which is averaged over the azimuth angle $\phi_{\mathbf{k}}$, to describe the kinetics of the density matrix with m=0. Accordingly, the KSBEs become

$$\partial_t \rho_{\mathbf{k}}^* + i \left[\frac{\Omega_z(\mathbf{k})}{2} \sigma_z, \rho_{\mathbf{k}}^* \right] + i \left[\frac{\Omega}{2} \sigma_x, \rho_{\mathbf{k}}^* \right] + i \left[\frac{\Omega_{\text{HF}}}{2} \cdot \boldsymbol{\sigma}, \rho_{\mathbf{k}}^* \right]$$

$$+ \sum_{\mathbf{k}'} W_{\mathbf{k}\mathbf{k}'}(\rho_{\mathbf{k}}^* - \rho_{\mathbf{k}'}^*) = 0.$$
(A3)

We then transform the KSBEs [Eq. (A3)] from the collinear space to the helix one by the transformation matrix

$$U_{\mathbf{k}} = \begin{pmatrix} \frac{-\Omega}{\sqrt{\Omega^2 + \Omega_{-}^2}} & \frac{-\Omega}{\sqrt{\Omega^2 + \Omega_{+}^2}} \\ \frac{\Omega_{-}}{\sqrt{\Omega^2 + \Omega_{-}^2}} & \frac{\Omega_{+}}{\sqrt{\Omega^2 + \Omega_{+}^2}} \end{pmatrix}, \quad (A4)$$

with $\Omega_{+} = \alpha k_x + \Omega_{\text{tot}}$ and $\Omega_{-} = \alpha k_x - \Omega_{\text{tot}}$. Here, $\Omega_{\text{tot}} = \sqrt{\Omega^2 + \alpha^2 k_x^2}$ is half of the total magnetic field. When the strong Zeeman magnetic field satisfies $|\Omega| \gg |\alpha k_x|$, Eq. (A4) can be simplified into

$$U_{\mathbf{k}} \approx \frac{1}{\sqrt{2}} \begin{pmatrix} A_{\mathbf{k}} - \frac{\alpha k_x}{2\Omega} & A_{\mathbf{k}} + \frac{\alpha k_x}{2\Omega} \\ A_{\mathbf{k}} + \frac{\alpha k_x}{2\Omega} & -A_{\mathbf{k}} + \frac{\alpha k_x}{2\Omega} \end{pmatrix}, \tag{A5}$$

with $A_{\mathbf{k}} \equiv -1 + \alpha^2 k_x^2/(8\Omega^2)$. After the transformation, the KSBEs in the helix space become

$$\partial_{t}\rho_{\mathbf{k}}^{h} + \frac{i}{2}\sqrt{\Omega^{2} + \alpha^{2}k_{x}^{2}}[\sigma_{z'}, \rho_{\mathbf{k}}^{h}]$$

$$+ i\frac{\Omega_{\mathrm{HF}}}{2}\cos(\Omega t)[\sigma_{y'}, \rho_{\mathbf{k}}^{h}] - i\frac{\Omega_{\mathrm{HF}}}{2}\sin(\Omega t)[\sigma_{x'}, \rho_{\mathbf{k}}^{h}]$$

$$+ \sum_{\mathbf{k'}} W_{\mathbf{k}\mathbf{k'}}(\rho_{\mathbf{k}}^{h} - \rho_{\mathbf{k'}}^{h})$$

$$+ \sum_{\mathbf{k'}} W_{\mathbf{k}\mathbf{k'}}\frac{\alpha^{2}(k_{x}' - k_{x})^{2}}{4\Omega^{2}}(\rho_{\mathbf{k'}}^{h} - \sigma_{y'}\rho_{\mathbf{k'}}^{h}\sigma_{y'})$$

$$+ \sum_{\mathbf{k'}} W_{\mathbf{k}\mathbf{k'}}\frac{i\alpha}{2\Omega}(k_{x} - k_{x}')[\sigma_{y'}, \rho_{\mathbf{k'}}^{h}] = 0, \tag{A6}$$

with the density matrix in the helix space with m=0 being $\rho_{\mathbf{k}}^h = U_{\mathbf{k}}^{\dagger} \rho_{\mathbf{k}}^* U_{\mathbf{k}}$.

Equations (A6) describe the kinetics of the density matrices in the helix space under the magnetic field $\Omega_{\rm tot}/2$ together with the rotating HF effective magnetic field. Moreover, in the helix space, the scattering terms include not only the spin-conserving part [the fifth and sixth terms in the left hand side (LHS) of Eq. (A6)], but also the effective spin-flip part [the last term in the LHS of Eq. (A6)].

We then transform the KSBEs into the interaction picture with the density matrix

$$\tilde{\rho}_{\mathbf{k}} = e^{i\Omega_{\mathrm{HF}}\sigma_{y'}t/2}e^{i\Omega\sigma_{z'}t/2}\rho_{\mathbf{k}}^{h}e^{-i\Omega\sigma_{z'}t/2}e^{-i\Omega_{\mathrm{HF}}\sigma_{y'}t/2}. \tag{A7}$$

Here, the density matrix can be expanded by the Legendre function

$$\tilde{\rho}_{\mathbf{k}} = \sum_{l} C_{l} \tilde{\rho}_{k,l} P_{l}(\cos \theta_{\mathbf{k}}), \tag{A8}$$

with $C_l = \sqrt{(2l+1)/(4\pi)}$. In the derivation below, the scattering matrix element $|U_{\mathbf{k}-\mathbf{k}'}|$ in $W_{\mathbf{k}\mathbf{k}'}$ is taken to be constant by considering the property of the interatom scattering potential [Eq. (4)]. By defining the spin vector $\tilde{\mathbf{S}}_{\mathbf{k}}^l = \text{Tr}[\tilde{\rho}_{k,l}\boldsymbol{\sigma}]$, taking the approximation $\sqrt{\Omega^2 + \alpha^2 k_x^2} \approx \Omega + \alpha^2 k_x^2/(2\Omega)$ and applying the rotation wave approximation $(|\Omega| \gg |\alpha k_x|)$, one obtains

$$\frac{\partial \tilde{\mathbf{S}}_{k}^{l}}{\partial t} + \frac{\Omega_{\text{so}}^{2}(\mathbf{k})}{2\Omega} U_{1}(t) \left[\frac{4l^{3} + 6l^{2} - 1}{(2l-1)(2l+1)(2l+3)} \tilde{\mathbf{S}}_{k}^{l} \right]
+ \sqrt{\frac{2l-3}{2l+1}} \frac{l(l-1)}{(2l-3)(2l-1)} \tilde{\mathbf{S}}_{k}^{l-2} + \sqrt{\frac{2l+5}{2l+1}}
\times \frac{(l+1)(l+2)}{(2l+3)(2l+5)} \tilde{\mathbf{S}}_{k}^{l+2} + U_{2}(t) \tilde{\mathbf{S}}_{k}^{l}
+ \frac{\sqrt{3}\Omega_{\text{so}}(\mathbf{k})}{3\Omega\tau_{k,1}} U_{3}(t) \left(\tilde{\mathbf{S}}_{k}^{0} \delta_{l1} - \tilde{\mathbf{S}}_{k}^{1} \delta_{l0} \right) = 0, \tag{A9}$$

with $\Omega_{\rm so}(\mathbf{k}) \equiv \alpha k$ and δ_{ij} being the Kronecker symbol. Here, the matrices $U_1(t)$ to $U_3(t)$ are defined by

$$U_1(t) = \begin{pmatrix} 0 & \cos(\Omega_{\rm HF}t) & 0\\ -\cos(\Omega_{\rm HF}t) & 0 & -\sin(\Omega_{\rm HF}t)\\ 0 & \sin(\Omega_{\rm HF}t) & 0 \end{pmatrix},\tag{A10}$$

$$U_{2}(t) = \begin{pmatrix} \frac{1}{\tau_{k,l}} + \frac{\Omega_{\text{so}}^{2}(\mathbf{k})}{4\Omega^{2}\tau_{k,1}} \delta_{l0} & 0 & 0\\ 0 & \frac{1}{\tau_{k,l}} + \frac{\Omega_{\text{so}}^{2}(\mathbf{k})}{6\Omega^{2}\tau_{k,1}} \delta_{l0} & 0\\ 0 & 0 & \frac{1}{\tau_{k,l}} + \frac{\Omega_{\text{so}}^{2}(\mathbf{k})}{4\Omega^{2}\tau_{k,1}} \delta_{l0} \end{pmatrix},$$
(A11)

and

$$U_3(t) = \begin{pmatrix} 0 & -\sin(\Omega t)\sin(\Omega_{\rm HF}t) & -\cos(\Omega t) \\ \sin(\Omega t)\sin(\Omega_{\rm HF}t) & 0 & -\sin(\Omega t)\cos(\Omega_{\rm HF}t) \\ \cos(\Omega t) & \sin(\Omega t)\cos(\Omega_{\rm HF}t) & 0 \end{pmatrix}. \tag{A12}$$

In Eq. (A9), when $\Omega_{\rm so}^2(\mathbf{k})\tau_{k,2}/(2\Omega) \ll 1$, we retain terms with $l \leq 2$. Specifically, in Eq. (A9), we have retained terms within the lowest two orders in the last two terms. By further applying the Markovian approximation, the tansverse spin vector in the interaction picture reads

$$\tilde{\mathbf{S}}_{k}^{0}(t) \approx p(\mathbf{k}) \exp\left[-t/\tau_{sz}(\mathbf{k})\right],$$
 (A13)

with $p(\mathbf{k}) = \text{Tr}[\rho_{\mathbf{k}}(0) \cdot \boldsymbol{\sigma}]/n_a$ being the initial spin vector for the atom with momentum \mathbf{k} . The transverse SRT $\tau_{sz}(\mathbf{k})$ is therefore

$$\tau_{sz}^{-1}(\mathbf{k}) = \frac{\Omega_{\text{so}}^{4}(\mathbf{k})\tau_{k,2}}{45\Omega^{2}(1+\Omega^{2}\tau_{k,2}^{2})} + \frac{\Omega_{\text{so}}^{2}(\mathbf{k})}{12\Omega^{2}} \left[\frac{(\Omega+\Omega_{\text{HF}})^{2}\tau_{k,1}}{1+(\Omega+\Omega_{\text{HF}})^{2}\tau_{k,1}^{2}} + \frac{(\Omega-\Omega_{\text{HF}})^{2}\tau_{k,1}}{1+(\Omega-\Omega_{\text{HF}})^{2}\tau_{k,1}^{2}} \right].$$
(A14)

By considering $|\Omega_{HF}| \ll |\Omega|$ in our derivation, the above equation is further simplified to be

$$\tau_{sz}^{-1}(\mathbf{k}) = \frac{\Omega_{so}^{4}(\mathbf{k})\tau_{k,2}}{45\Omega^{2}(1 + \Omega_{HF}^{2}\tau_{k,2}^{2})} + \frac{\Omega_{so}^{2}(\mathbf{k})\tau_{k,1}}{6(1 + \Omega^{2}\tau_{k,1}^{2})}.$$
 (A15)

- * Author to whom correspondence should be addressed; Electronic address: mwwu@ustc.edu.cn.
- Y. J. Lin, R. L. Compton, A. R. Perry, W. D. Phillips, J. V. Porto, and I. B. Spielman, Phys. Rev. Lett. 102, 130401 (2009).
- ² R. A. Williams, L. J. LeBlanc, K. J. García, M. C. Beeler, A. R. Perry, W. D. Phillips, and I. B. Spielman, Science 335, 314 (2012).
- ³ M. Aidelsburger, M. Atala, S. Nascimbène, S. Trotzky, Y. A. Chen, and I. Bloch, Phys. Rev. Lett. **107**, 255301 (2011).
- ⁴ S. Simonucci, G. Garberoglio, and S. Taioli, Phys. Rev. A 84, 043639 (2011).
- ⁵ Y. J. Lin, K. J. García, and I. B. Spielman, Nature(London) 471, 83 (2011).
- ⁶ P. Wang, Z. Q. Yu, Z. Fu, J. Miao, L. H. Huang, S. J. Chai, H. Zhai, and J. Z, Phys. Rev. Lett. **109**, 095301 (2012).
- ⁷ L. W. Cheuk, A. T. Sommer, Z. Hadzibabic, T. Yefsah, W. S. Bakr, and M. W. Zwierlein, Phys. Rev. Lett. **109**, 095302 (2012).
- ⁸ T. D. Stanescu, B. Anderson, and V. Galitski, Phys. Rev. A **78**, 023616 (2008).
- ⁹ C. Wang, C. Gao, C. M. Jian, and H. Zhai, Phys. Rev. Lett. **105**, 160403 (2010).
- ¹⁰ T. L. Ho and S. Zhang, Phys. Rev. Lett. **107**, 150403 (2011).

- ¹¹ C. M. Jian and H. Zhai, Phys. Rev. B **84**, 060508(R) (2011).
- H. Hu, B. Ramachandhran, H. Pu, and X. J. Liu, Phys. Rev. Lett. 108, 010402 (2012).
- $^{13}\,$ T. Schäfer, Phys. Rev. A $\bf 85,\,033623$ (2012).
- ¹⁴ Z. F. Xu, Y. Kawaguchi, L. You, and M. Ueda, Phys. Rev. A 86, 033628 (2012).
- ¹⁵ T. Ozawa and G. Baym, Phys. Rev. Lett. **110**, 085304 (2013).
- ¹⁶ C. Qu, C. Hamner, M. Gong, C. W. Zhang, and P. Engels, Phys. Rev. A 88, 021604(R) (2013).
- ¹⁷ I. Bloch, J. Dalibard, and W. Zwerger, Rev. Mod. Phys. 80, 885 (2008).
- ¹⁸ I. V. Tokatly and E. Ya. Sherman, Phys. Rev. A 87, 041602(R) (2013).
- ¹⁹ S. S. Natu and S. D. Sarma, Phys. Rev. A 88, 033613 (2013).
- ²⁰ J. Y. Zhang, S. C. Ji, Z. Chen, L. Zhang, Z. D. Du, B. Yan, G. S. Pan, B. Zhao, Y. J. Deng, H. Zhai, S. Chen, and J. W. Pan, Phys. Rev. Lett. **109**, 115301 (2012).
- Y. Zhou, T. Yu, and M. W. Wu, Phys. Rev. B 87, 245304 (2013).
- ²² Y. Yafet, Phys. Rev. **85**, 478 (1952).
- ²³ R. J. Elliott, Phys. Rev. **96**, 266 (1954).
- ²⁴ M. I. D'yakonov and V. I. Perel', Zh. Eksp. Teor. Fiz. **60**, 1954 (1971) [Sov. Phys. JETP **33**, 1053 (1971)].

- ²⁵ G. Dresselhaus, Phys. Rev. **100**, 580 (1955).
- ²⁶ Y. A. Bychkov and E. I. Rashba, J. Phys. C **17**, 6039 (1984); Pis'ma Zh. Eksp. Teor. Fiz. **39**, 66 (1984) [JETP Lett. **39**, 78 (1984)].
- ²⁷ M. W. Wu, J. H. Jiang, and M. Q. Weng, Phys. Rep. **493**, 61 (2010).
- ²⁸ M. Q. Weng and M. W. Wu, Phys. Rev. B **68**, 075312 (2003).
- ²⁹ D. Stich, J. Zhou, T. Korn, D. Schulz, R. Schuh, W. Wegscheider, M. W. Wu, and C. Schüller, Phys. Rev. Lett. **98**, 176401 (2007); Phys. Rev. B **76**, 205301 (2007).
- ³⁰ T. Korn, D. Stich, R. Schulz, D. Schuh, W. Wegscheider, and C. Schüller, Adv. Solid State Phys. 48, 143 (2009).
- ³¹ F. Zhang, H. Z. Zheng, Y. Ji, J. Liu, and G. R. Li, Europhys. Lett. 83, 47006 (2008).
- ³² C. A. Regal, C. Ticknor, J. L. Bohn, and D. S. Jin, Phys. Rev. Lett. **90**, 053201 (2003).
- ³³ M. Egorov, B. Opanchuk, P. Drummond, B. V. Hall, P. Hannaford, and A. I. Sidorov, Phys. Rev. A 87, 053614 (2013).
- ³⁴ T. Ozawa, L. P. Pitaevskii, and S. Stringari, Phys. Rev. A 87, 063610 (2013).
- ³⁵ R. A. Williams, M. C. Beeler, L. J. LeBlanc, K. J. García, and I. B. Spielman, Phys. Rev. Lett. **111**, 095301 (2013).
- M. W. Wu and C. Z. Ning, Eur. Phys. J. B. 18, 373 (2000);
 M. W. Wu, J. Phys. Soc. Jpn. 70, 2195 (2001).
- ³⁷ M. W. Wu and H. Metiu, Phys. Rev. B **61**, 2945 (2000).
- ³⁸ H. Haug and A. P. Jauho, Quantum Kinetics in Transport and Optics of Semiconductors (Springer, Berlin, 1996).
- ³⁹ J. H. Jiang and M. W. Wu, Phys. Rev. B **79**, 125206 (2009).
- ⁴⁰ Semiconductor Spintronics and Quantum Computation, edited by D. D. Awschalom, D. Loss, and N. Samarth (Springer, Berlin, 2002).
- ⁴¹ I. Žutić, J. Fabian, and S. D. Sarma, Rev. Mod. Phys. **76**, 323 (2004).
- ⁴² J. Fabian, A. M. Abiague, C. Ertler, P. Stano, and I. Žutić, Acta Phys. Slov. **57**, 565 (2007).
- ⁴³ Spin Physics in Semiconductors, edited by M. I. D'yakonov (Springer, Berlin, 2008).

- ⁴⁴ T. Korn, Phys. Rep. **494**, 415 (2010).
- ⁴⁵ F. Meier and B. P. Zakharchenya, Optical Orientation (North-Holland, Amsterdam, 1984).
- The total spin vectors [Eqs. (11) and (12)] and the SRTs [Eqs. (13) and (14)] for the transverse and longitudinal spin relaxations were originally obtained in the two-dimensional system. However, they are still valid in the three-dimensional situation, because the effective magnetic field in Eq. (2) only depends on the magnitude of the momentum \mathbf{k} and the zenith angle $\theta_{\mathbf{k}}$ between \mathbf{k} and the \hat{x} -axis, but not on the azimuth angle $\phi_{\mathbf{k}}$ between \mathbf{k} and \hat{y} -axis in the y-z plane. Accordingly, the KSBEs can be reduced to the same form as that in the two-dimensional system by averaging the density matrix on $\phi_{\mathbf{k}}$ [see also Eq. (A3) in Appendix A].
- ⁴⁷ C. Grimaldi, Phys. Rev. B **72**, 075307 (2005).
- ⁴⁸ If the first term in Eq. (23) is dominant, the SRT shows a platform in the scattering length dependence.
- ⁴⁹ Under the unique effective magnetic field $\Omega(\mathbf{k}) = (\Omega, 0, \alpha k_x)$ with $|\Omega| \ll \langle |\Omega_z(\mathbf{k})| \rangle$, the spin polarization, i.e., the HF effective magnetic field is roughly along the \hat{z} -axis. Therefore, when $|\Omega_{\rm HF}| \ll \langle |\Omega_z(\mathbf{k})| \rangle$, the HF effective magnetic field has little influence on the spin relaxation. Indeed, if we remove the HF magnetic field in the computation at this regime, the SRT changes little. By solving the KSBEs [Eq. (9)] with the HF effective magnetic field and the scattering term neglected, one finds the spin vector along the \hat{z} -direction

$$S_z(t) = \sum_{\mathbf{k}} \frac{p(\mathbf{k})}{\alpha^2 k_x^2 + \Omega^2} \left(\Omega^2 \cos(\sqrt{\alpha^2 k_x^2 + \Omega^2} t) + \alpha^2 k_x^2 \right),$$

with $p(\mathbf{k}) = \text{Tr}[\rho_{\mathbf{k}}(0) \cdot \boldsymbol{\sigma}]/n_a$ being the initial spin vector for the atom with momentum \mathbf{k} . Accordingly, when the population for the atoms in \mathbf{k} -space is broadened, the inhomogeneous broadening $\langle \alpha^2 k_x^2 \rangle$ is enhanced.

H. Haug and S. W. Koch, Quantum Theory of the Optical and Electronic Properties of Semiconductors (World Scientific, Singapore, 2004), 4rd ed.